ar-12-0954-R1 clean copy

Differentially expressed epigenome modifiers, including Aurora kinase A and B, in immune cells of rheumatoid arthritis

Tibor T. Glant, MD, PhD[1-3], Timea Besenyei, MD[1], András Kádár, MD[1], Júlia Kurkó, MD[1], Beata Tryniszewska, MS[1], János Gál, MD[4], Györgyi Soós, MD[5], Zoltán Szekanecz, MD, PhD[6], Gyula Hoffmann, PhD[7], Joel A. Block, MD[3], Robert S. Katz, MD[3], Katalin Mikecz, MD, PhD[1,2], and Tibor A. Rauch, PhD*[1]

Section of Molecular Medicine, Departments of [1]Orthopedic Surgery, [2]Biochemistry, [3]Internal Medicine (Section of Rheumatology and Rheumatology Associates), Rush University Medical Center, Chicago, IL 60612, USA; [4]Department of Rheumatology, [5]Genetic Laboratory of County Hospital, Kecskemét, Hungary; County Hospital, [6]Department of Rheumatology, Medical and Health Science Center, Debrecen, Hungary; [7]Department of Genetics and Molecular Biology, University of Pécs, Hungary.

Running Title: Epigenome modifiers in rheumatoid arthritis

***Address correspondence to:**

Tibor A. Rauch, PhD, Section of Molecular Medicine, Department of Orthopedic Surgery, Rush University Medical Center, 1735 W. Harrison St, Chicago, IL 60612. Phone: 1-312-942-5766; Fax: 1-312-942-8828; E-mail: Tibor_Rauch@rush.edu

Funding sources: This study was supported in part with grants from the National Institutes of Health (AR059356), The Searle Foundation sponsored RTSC Pilot Grant, J.O. Galante MD, DMSc Chair of Orthopedic Surgery (Rush University Medical Center, Chicago, IL), and The Grainger Foundation (Lake Forest, IL).

ABSTRACT

Objective. The aim of this study was to identify epigenetic factors that are implicated in the pathogenesis of rheumatoid arthritis (RA) and to explore the therapeutic potential of the targeted inhibition of these factors.

Methods. PCR arrays were utilized to investigate the expression profile of genes that encod key epigenetic regulator enzymes. Mononuclear cells from RA patients and mice were monitored for gene expression changes, in association with arthritis development in murine models of RA. Selected genes were further characterized by quantitative real-time PCR, Western blot and flow cytometry methods. The targeted inhibition of the upregulated enzymes was studied in arthritic mice.

Results. A set of genes with arthritis-specific expression was identified by the PCR arrays. Aurora kinase A and B, both of which were highly expressed in arthritic mice and treatment naïve RA patients, were selected for detailed analysis. Elevated Aurora kinase expression was accompanied with an increased phosphorylation of histone H3, which promotes proliferation of T lymphocytes. Treatment with VX-680, a pan-Aurora kinase inhibitor, promoted B cell apoptosis, provided significant protection against the onset, and attenuated the inflammatory reactions in arthritic mice.

Conclusions. Arthritis development is accompanied the changes in the expression of a number of epigenome-modifying enzymes. Drug-induced downregulation of the Aurora kinases, among other targets, seems to be sufficient to treat experimental arthritis. Development of new therapeutics that target the Aurora kinases can potentially improve RA management.

INTRODUCTION

Rheumatoid arthritis (RA) is an inflammatory autoimmune disease that primarily targets the synovial joints (1). RA is a polygenic disease with strong immunogenetic components, although environmental and epigenetic factors may also contribute to the etiology (2). Therefore, enzymes that play a role in chromatin modification may be involved in the process that leads to RA and are plausible targets for therapy. RA is thought to be a T cell-dependent and B cell-mediated autoimmune disease. In cases where anti-TNF therapy has failed, treatment with a B cell-specific anti-CD20 antibody (i.e., Rituximab) conveyed beneficial effects by depleting B cells in patients with RA (3). Chromatin-modifying enzymes are involved in writing, decoding and erasing the epigenetic signals that are involved in various autoimmune diseases and tumor biology (4), but the clinical relevance of these enzymes is unknown in RA.

The Aurora kinases belong to the serine/threonine kinase superfamily and are involved in the regulation of cell proliferation (5). Three Aurora kinases have been identified in mammals, and all of them play a role in cell division by regulating various steps in centrosome formation and chromosome segregation (6) and they interact with a broad spectrum of phosphorylated partners that include histone H3 (7). Aurora kinase-specific inhibitors are implicated as anticancer drugs.

We identified changes in the expression of a number of epigenetic modifiers that are associated with arthritis both in mice and patients with RA. We also examined the molecular function of Aurora kinases in arthritis and tested the therapeutic potential of a kinase inhibitor VX-680 in a mouse model of RA.

Keywords: Aurora kinase, autoimmunity, rheumatoid arthritis, epigenetics, animal model,

MATERIALS AND METHODS

Mice

Retired breeder female BALB/c mice were purchased from the National Cancer Institute (NCI, Frederick, MD) and were used for the generation of cartilage proteoglycan (PG) aggrecan-induced arthritis (PGIA) according to a standard protocol (8,9). Briefly, the mice were immunized with PG purified from knee joint cartilage of osteoarthritic patients who had undergone joint replacement surgery. PG was injected intraperitoneally (i.p.) three times (at three-week intervals, 100 μg PG core protein/injection) with 2 mg of dimethyldioctadecyl-ammonium bromide (DDA) adjuvant into BALB/c mice (9,10). Mice were assessed for arthritis in the limbs three times a week and were scored on a visual scale of 0 to 4 for each paw, thus yielding a maximum severity score of 16 for each mouse (8-11). To measure the therapeutic effect of VX-680 treatment on established arthritis, a microcaliper was used for measuring the thickness of the arthritic joints (11). Collagen-induced arthritis (**CIA**) was generated by immunizing male DBA/1J mice (The Jackson Laboratory, Bar Harbor, ME) with 100 μg of human type II collagen (CII) in complete or incomplete Freund's adjuvant following the standard CIA protocol (11-13). DBA/2 mice (NCI) that are resistant to both PGIA and CIA were immunized with either cartilage PG or CII as described above. Serum samples were harvested prior to the treatment with VX-680 and at the end of experiment (on day 17-18 of treatments). IgG1 and IgG2a isotypes of autoantibodies (anti-mouse PG) were measured in serum samples of BALB/c mice (8-10,12,14). Animal experiments were approved by the Institutional Animal Care and Use Committee, and human studies by the Institutional Review Board at Rush University Medical Center, Chicago, IL, USA.

VX-680 treatment of BALB/c mice with PGIA

In general, arthritis develops 9-10 days after the third PG-immunization. *Prophylactic* preventive treatment with VX-680 was initiated six days prior to the expected onset of PGIA. Mice were i.p. injected with 40 mg/kg of VX-680 (Sellekchem, Houston, TX), which is an effective dose described for cancer treatment (15), and which did not affected the viability of cells harvested by peritoneal lavage (data not shown). VX-680 was dissolved in dimethyl sulfoxide (DMSO, 100 mg/ml) and diluted in 25% isopropyl alcohol. VX-680 was administered each day during the first week of the experiment and then every other day until the animals were sacrificed. *For therapeutic treatment,* arthritic BALB/c mice were i.p. injected with 50 mg/kg of VX-680. Prior to the treatment, arthritic mice were selected to have approximately the same cumulative arthritis scores (~2.5 ±1.0, n= 8-10). The mice received the first VX-680 treatment after the first symptoms (redness and swelling of the paws) of arthritis were observed and then received treatment every other day until the animals were sacrificed.

RNA isolation, cDNA synthesis, and quantitative real-time polymerase chain reaction (qRT-PCR)

Cells were collected from the spleens, bone marrow, and joint draining lymph nodes (LNs) on day 17 after the third PG injection. Before the purification of lymphocytes, aliquots of the spleen, bone marrow and LN cells were used for RNA isolation. T and B cells were purified using antibody-coated magnetic beads (StemCell Technologies, Vancouver, BC, Canada). The RNA was isolated from aliquots of spleen cells and purified lymphocytes using a TRI reagent (Sigma-Aldrich, St. Louis, MO) immediately after the separation or purification. One µg of the total RNA was used for cDNA synthesis using iScript kit (Bio-Rad, Hercules, CA). qRT-PCR was performed using an iQ5 RT-PCR machine (Bio-Rad) and the SsoFast™ EvaGreen® Supermix (Bio-Rad). The primers were designed using PrimerQuest software and were manufactured by Integrated DNA Technologies (Coralville, IA). The qRT-PCR primer sequences

are available upon request. The specificity of the qRT-PCR product was monitored by a post-PCR melting curve analysis (16). Samples were tested in triplicate, and the iQ5 PCR software was used to calculate the normalized fold expression changes based on the ΔC_t method. Measured C_t values were normalized to the *β-actin* or *Gapdh* internal control values. The PBMCs from the blood samples from consenting, healthy individuals and disease modifying anti-rheumatic drug (DMARD) treatment naïve RA patients (Supplementary Table 1) were separated on a Ficoll gradient within one hour after blood collection. The isolated mononuclear cells were stored in RNAlater® (Ambion/LifeTechnologies, Grand Island, NY) until the RNA preparation was performed. The cDNA synthesis and qRT-PCR were performed as described for the mouse samples.

PCR arrays

Human (PHS-085) and mouse (PMM-085) "RT^{2}Profiler™" PCR arrays (SABioscience, Fredrick, MD) were used for the study of arthritis-associated changes in the expression of 84 chromatin-modifying enzymes. We used the company's reagents for cDNA synthesis and followed the manufacturer's instructions for qRT-PCR.

Western blot analysis

For Western blot analysis, we used the same cells as those isolated for the total RNA preparation. Cell extracts were prepared in RIPA buffer (17) with Protease Inhibitor Cocktail® (Roche, Indianapolis, IN). Protein concentrations were determined using the BCA Protein Assay kit™ (Pierce, Rockford, IL)., Proteins (30 µg/lane) were resolved using 8% SDS-polyacrylamide gel electrophoresis (PAGE) and transferred onto nitrocellulose membranes (Bio-Rad). The membranes were blocked with 5% bovine serum albumin (Sigma-Aldrich) in phosphate-buffered saline (PBS, pH 7.5) for 1 hour and then

incubated with primary antibodies at 4°C overnight. The following primary antibodies were used: rabbit polyclonal anti-Aurora A (ab61114, Abcam, Cambridge, UK), rabbit polyclonal anti-Aurora B (#3094, Cell Signaling Technology, Beverly, MA) and mouse monoclonal (mAb) anti-Gapdh (clone 6C5, Abcam). Peroxidase-conjugated secondary antibodies were purchased from Santa Cruz Biotechnology (Santa Cruz, CA). Western blots were developed using Plus Western Blotting Substrate (Pierce).

The histone fractions were prepared from purified B cells (17) and were resolved on a12% SDS-PAGE gel. Immune detection of the phosphorylation-modified or un-modified histone H3 was performed as described above (17). The primary antibodies were rabbit polyclonal antibodies against phosphorylated Histone H3 Ser10 (H.H3-P, ab5176) or histone H3 (H.H3, ab1791) both from Abcam.

Tissue culture

For the apoptosis-related gene expression studies, spleen cells from mice with PGIA were cultured in 24-well tissue culture plates for 3 days in Dulbecco's Modifed of Eagle's Medium (DMEM) supplemented with 10% fetal bovine serum (FBS). The cells were treated with 60, 300 or 1500 nM VX-680 or mock-treated with DMSO (15). RNA was isolated daily from the treated spleen cells on the three subsequent days. The expression levels of the *p53* and *Puma* genes were measured using qRT-PCR.

Flow cytometry

T and B cells isolated from the spleens, lymph nodes, or bone marrow of mice were analyzed using multicolor flow cytometry. Briefly, 10^6 cells/well were seeded into 96-well U-bottom plates (BD Falcon), and the Fc receptors were blocked with anti-CD16/CD32 mAb (BioLegend, San Diego, CA) for 15 minutes at 4^oC. The samples were incubated with fluorochrome-conjugated mAbs against mouse CD3, CD19, active caspase 3, IgM, IgD, or CD138 (mAbs from BioLegend or BD Biosciences, San

Diego, CA) in 100 µl of flow cytometry staining/washing buffer (0.1% bovine serum albumin in PBS with 0.1% NaN_3) for 30 min in the dark at 4^{o}C. The cells were washed twice and analyzed on the same day. Data acquisition and analysis were performed using a FACS Canto II flow cytometer with an HTS module and FACS DIVA software (BD Flow Cytometry Systems, San Jose, CA). Initial gating was performed on lymphoid cells (based on the forward/side scatter (FSC/SSC) parameters). The $CD19^+$ cells were defined as total B cells and the $CD3^+$ cells were defined as total T cells. Intracellular caspase 3 was detected after permeabilization with Cytofix/Cytoperm (BD Biosciences). B cell subsets were analyzed after co-staining with anti-CD19, anti-IgM, and anti-IgD mAbs (B1 and B 2 cells), or with anti-CD19 and anti-CD138 mAbs (plasmablasts/plasma cells) (18).

Statistical analysis

Descriptive statistics were used to determine the group means and the standard error of the mean (mean ± SEM), unless otherwise stated. The difference between two groups was tested for statistical significance using a Student's t-test. When non-parametric distribution occurred (e.g., human samples), we used Mann-Whitney U test to compare results. $P \leq 0.05$ was considered to be statistically significant.

RESULTS

A subset of chromatin-modifying enzymes shows disease-associated changes in expression in arthritic mice and RA

To explore the chromatin-modifying factors that are implicated in the pathogenesis of arthritis, we used PCR arrays to detect the expression of 84 genes that encode key enzymes that are known to be specific chromatin modifiers (Figure 1A). Changes in gene expression were investigated in RNA samples purified from spleen cells of control mice and cartilage proteoglycan (PG)-immunized arthritic mice (PG-induced arthritis, PGIA). We detected 2.58- to 4.44-fold increases in the expression of six

genes, and nine genes showed decreased expression (2.15- to 4.60-fold downregulation) in mice with PGIA (Figure 1A and Supplementary Table 2). We used an analogous human PCR array to investigate the expression of similar genes using RNA samples purified from PBMCs of DMARD treatment-naive RA patients (Figure 2A). In this introductory study, we selected Aurora kinase A and B for further analyses, both of which showed greater than two-fold upregulation in all of the patients tested (Supplementary Figure 1 and Supplementary Tables 2 and 3). We detected upregulation of nine genes in the PBMCs of these RA patients. Increased expression of four of these genes (i.e., *AURKA, AURKB, ESCO2* and *NEK6*) was also detected in mice with acute arthritis (Figure 2A and Supplementary Tables 2 and 3). The PCR array data were verified by qRT-PCR experiments that showed 2.8- to 4.2-fold upregulation of both Aurora kinases ($P<0.01$) and 1.5- to 3.5-fold upregulation of the other genes (Figure 2B and Supplementary Figure 1). Five additional genes showed significant repression in RA patients when compared to healthy individuals. Two of the downregulated genes (i.e., *HDAC1* and *SETDB2*) were also found to undergo similar regulation in mice with PGIA (Supplementary Tables 2 and 3).

We have chosen the Aurora kinases for further analyses because these are the best-characterized histone-modifying enzymes among the genes identified in our study. We investigated the expression of the two Aurora kinases in low-dose methotrexate (MTX)-treated patients and found that both were significantly downregulated following MTX treatment (Figure 2C). These data suggested that Aurora kinase A and B play pivotal roles in the pathogenesis of RA, and their downregulation may be a key factor in successful arthritis therapy with MTX.

Because it was unclear which cell type(s) displays altered Aurora kinase expression in arthritis (Figures 1B and 2B), we employed a murine model (PGIA) of RA. The PGIA model exhibits many symptoms and produces biomarkers of RA (10) that are included in the diagnostic criteria of the human

disease (19). We separated B and T lymphocytes and found similar results in both cell types, although expression levels were lower in T cells (Supplementary Figure 2 and Supplementary Table 2). Thus, we concluded that B lymphocytes might be the dominant mononuclear cell type that expresses high levels of the Aurora kinases in arthritis. To test this hypothesis, additional experiments were performed with purified B cells isolated from control and arthritic mice. In addition to spleen cells, we investigated the expression level of Aurora kinases in bone marrow and joint draining LNs, and found significant upregulation of both enzymes in the bone marrow but not in the LNs of mice with PGIA (Supplementary Figure 3).

Phosphorylation of histone H3 by the Aurora kinases in arthritis

Although histone H3 phosphorylation at serine 10 can be performed by RPS6KA5 (20) and CHUK (21) kinases we could not detect significant expression changes for these enzymes. To investigate whether the increased expression of the Aurora kinases resulted in elevated protein levels, we performed a Western blot analysis using kinase-specific antibodies and cell lysates from mouse B lymphocytes (Figure 1C). Strong kinase-specific signals were observed in purified B cell lysates from arthritic mice; however, these signals were almost undetectable in cell lysates from the control (adjuvant-treated) mice (Figure 1C). To assess enzymatic activity, we exploited the fact that Aurora kinase A and B selectively interact with and phosphorylate histone H3 on serine 10 (7) (Figure 1D). The phosphorylation level of serine 10 was at least 7 times higher in arthritic mice compared to control mice. The phosphorylation of histone H3 results in chromatin condensation and subsequent mitosis in arthritic mice. These data are consistent with elevated B cell activity that is characteristic for the acute phase of polyarthritis (22-25).

Elevated expression of Aurora kinases is associated with the onset of arthritis

Although we detected elevated expression of Aurora kinases during the acute phase of PGIA in BALB/c mice, it was still unknown whether these changes were specific for lymphocyte activation and/or inflammation in arthritis. The BALB/c mouse strain is highly susceptible to PGIA and resistant to collagen II (CII)-induced arthritis (CIA); however, an immune reaction to CII can be provoked in these mice by immunization with CII (14). Reciprocally, the DBA/1J mouse strain is susceptible to CIA but resistant to PGIA. BALB/c mice were immunized with human PG or CII, and the expression levels of Aurora kinase A and B were measured using qRT-PCR (Figures 3A and 3B). Following the first injection of CII, the expression rate of both Aurora kinases increased moderately. Subsequent immunizations did not change the expression levels, which gradually returned to baseline levels by week seven (Figures 3A and 3B). The Aurora kinase expressions were markedly different in BALB/c mice in response to PG immunization provoking a gradual increase of kinase expression. Expression levels reached their peak at the onset of arthritis (Figures 3A and 3B). The pattern of Aurora kinase expression was confirmed in the CIA model in DBA/1J mice. The level of both Aurora kinase transcripts increased gradually in the mice with increased symptoms of CIA (Figures 3C and D). Finally, we tested whether PG immunization could induce an increase in the expression of the Aurora kinases in PGIA- and CIA-resistant DBA/2 mice. Although a mild increase was detected, this expression was notably lower than that observed for the BALB/c mice that were immunized with either PG or CII (data not shown). Taken together, the very high expression of the Aurora kinases is characteristic of the onset of arthritis and is associated with the acute phase of polyarthritis in animal models of RA and in treatment-naive RA patients.

We extended our experiments to examine the chronic phase of the disease by determining at later time points in PGIA. As shown in Figure 3E, expression of the Aurora kinases continually increased,

and reached a peak just before or at the time of the onset of arthritis. However, expression levels dropped to baseline levels in the chronic phase of the disease (Figure 3E).

Preventive and therapeutic treatment of PGIA mice with the pan-Aurora kinase inhibitor VX-680

VX-680 is a specific inhibitor of both Aurora kinases (26) and results in polyploidy that ultimately induces cell death by apoptosis (27). First, we investigated the effects of VX-680 on cultured splenocytes that were isolated from arthritic BALB/c mice. VX-680 treatment at 300 μM induced elevated expression of the apoptosis-promoting transcription factor *p53* and the *Puma* genes (28), which was accompanied by decreased viability of splenocytes (Supplementary Figure 4).

We next investigated the preventive effect of VX-680 on arthritis development in PGIA mice (Figure 4). We started VX-680 treatment six to seven days prior to the expected onset of arthritis and continued treatment until the end of the experiment (Figure 4A). qRT-PCR and histone phosphorylation assays demonstrated that VX-680 treatment reduced both the expression and activity of the two Aurora kinases (Figures 4B-4D). The total B cell numbers ($CD19^+$) were significantly decreased in the treated animals (49.2 ± 1.3% to 38.4 ± 2.8%; P = 0.0044).

To evaluate the potential of VX-680 to treat PGIA, arthritic mice were injected i.p. with either VX-680 or vehicle every other day following the first signs of arthritis (Figure 5). Swelling of the peripheral joints was significantly reduced in the VX-680-treated animals compared to the vehicle-treated controls. Downregulation of the Aurora kinase genes was associated with reduced phosphorylation of the histone substrates (Figures 5B and C). At the end of the therapeutic treatment (day 11), we detected an elevated number of active caspase 3^+ B lymphocytes, indicating the induction of apoptotic events in the B cells by VX-680 (Figures 6A and B). Overall, the drug treatment increased the number of apoptotic $CD19^+$ cells from 4.66 ± 1.88% to 28.57 ± 3.5% (P = 0.00048), and the total B

cell number was 30% less in the VX-680-treated animals (47 ± 5.4%) compared to the vehicle-treated mice (76.9 ± 2.2%) (P = 0.0068). The proportion of intracellular active caspase 3^+ B lymphocytes, but not T cells, was elevated in the spleens of VX-680- treated mice (Figure 6A-D). B cell loss (involving both B1 [IgM high/IgD low] and B2 [IgD high/IgM low] subsets) was detected in the spleens (Figure 6F), and bone marrow (Figure 6G), but not in the LNs (Figure 6F). The proportions of $CD19^+CD138^+$ B cells (antibody-secreting plasmablasts and plasma cells) were not reduced in these organs in the VX-680-treated mice (data not shown).

DISCUSSION

The most extensive information regarding epigenetics in RA is from studies that have focused on RA synovial fibroblasts (29). Activated synovial fibroblasts were characterized by alterations in global DNA methylation levels (30) (i.e., hypomethylation) and the elevated expression of certain histone modifiers (31,32). These modifiers increase the production of pro-inflammatory cytokines, thus promoting the migration of immune cells into inflamed joints (33). In the present work, we have identified a number of genes that show arthritis-specific expression in mononuclear cells isolated from arthritic animals and RA patients (Supplementary Tables 2 and 3). Most of these genes have been studied in the context of carcinogenesis, but their implication in the pathogenesis of arthritis is novel and has not been investigated. We found several dozen genes that were significantly up- or downregulated in arthritis. For the first time, we have identified all of the major chromatin-modifying enzyme families that can be implicated in autoimmune arthritis (Figures 1 and 2). These "arthritis-specific" genes include those encoding histone kinases (*AURKA*, *AURKB* and *NEK6*), acetyltransferases (*ESCO2* and *KAT2B*), deacetylases (*HDAC1* and *HDAC11*), methyltransferases (*SETD6, SETDB2* and *PRMT6*), demethylases

(*KDM5C* and *KDM6B*) and protein degradation-promoting ubiquitin ligases (*DZIP3* and *UBE2B*). Many of these genes and their corresponding enzyme products have activating or repressing functions that directly or indirectly modulate the activity of the NF-κB transcription factor. This information represents the most obvious link to arthritis, a disease controlled by a number of NF-κB-regulated pro-inflammatory cytokines. Specifically, H.H3-P is an important epigenetic signal for the recruitment of NF-κB to the promoters of a number of cytokine genes (34).

Another observation that supports the modulation of NF-κB signaling in arthritis is the downregulation of *SETD6*, which is a known negative regulator of NF-κB signaling (35). The pathological relevance of SETD6 is further supported by the fact that it can interact with NEK6 and the Aurora kinases (36), enzymes that we identified as arthritis-promoting genes.

Other genes, such as *HDAC11* and *KDM6B,* may affect inflammatory pathways. Overexpression of *HDAC11* (an inhibitor) suppresses IL-10 (an anti-inflammatory cytokine), thus enhancing antigen presentation (37) and promoting arthritis. Finally, there is a number of other genes that were identified for which the direct targets in mononuclear cells are still unknown. For example, overexpression of *KDM6B*, which can eliminate strong repressive epigenetic transcription signals (i.e., histone H3 K27 tri-methylation), has been implicated in macrophage activation (38). Although all of the enzymes discussed above are primarily considered to be histone modifiers, a number of studies have shown that other intracellular proteins may also be targets of these enzymes. For example, NEK6 can phosphorylate the STAT3 transcription factor (39) that plays a role in the induction of the IL-6 family of cytokines (40,41). Therefore, a complete understanding of the epigenetic components of arthritis requires the identification of target genes and the characterization of the intricate regulatory networks that exist among these enzymes. Our work took the first steps in this direction by exploring and implicating a set of epigenetically relevant genes in arthritis.

Using different mouse models of RA, we have proven that the increased expression of the Aurora kinases is specific to arthritis and is not associated with normal physiological lymphocyte activation and differentiation. Pathologically high Aurora kinase expression is most prominent in the B cells. Aurora kinase expression was also increased in mouse T cells, but the levels observed in T cells were approximately half of those detected in B cells. Aurora kinase A and B expression progressively increased in the B cells prior to the onset of arthritis, and their levels reached a plateau at the onset of disease. Here, we demonstrated that increased Aurora kinase expression was associated with the elevated phosphorylation of histone H3; however, we assume that other kinase-interacting partners could also be modified. Because the Aurora kinases are involved in the regulation of certain NF-κB-controlled genes (34), it is reasonable to hypothesize that they may play multiple roles in the pathogenesis of arthritis. Targeted inhibition of the Aurora kinases with VX-680 delayed the onset of disease, and the therapeutic application of VX-680 significantly reduced the severity of arthritis. We have shown that VX-680 treatment induces B cell apoptosis, thus promoting B cell elimination in arthritic mice. The significance of these findings is underscored by the fact that the application of B cell-targeted therapy using an anti-CD20 antibody is a relatively new and effective treatment option for RA patients who are resistant to anti-TNF therapy (42,43). B cell apoptosis was not associated with significant decrease in the levels of autoantibody isotypes, most likely due to the long half-life of autoantibodies in the circulation. To prove this, however, a much longer period of treatment would be necessary or adaptive transfer of VX-680-treated B cells to antibody secretion-deficient mice, which is beyond the scope of the current study. Notably, we detected a 2-fold upregulation of the Aurora kinases in mouse T cells, but VX-680 treatment did not promote a significant level of apoptosis in T cells, which may be explained by the presence of additional anti-apoptotic factors that override the VX-680 effect in activated T cells. We observed high expression of Aurora kinases in the mononuclear cells from

untreated RA patients, but reduced expression of these kinases occurred in RA patients following MTX treatment. The observation that Aurora kinase expression was reduced in low-dose MTX-treated RA patients and in VX-680-treated arthritic mice suggests that the inhibition of these kinases is a promising step in pharmacological intervention. Although MTX and VX-680 have different molecular targets, we cannot exclude the possibility that some common pathogenic pathways are targeted. MTX is one of the most frequently used DMARDs in RA therapy (44). However, a large number of patients are resistant to MTX, and unpredictable side effects can occur (45). Therefore, the discovery and characterization of new drugs with similar therapeutic efficacy but different, or partially overlapping targets that are involved in the development of disease, can potentially improve the clinical management of RA.

ACKNOWLEDGEMENT

This study was supported in part with grants from the National Institutes of Health (AR059356), The Searle Foundation sponsored RTSC Pilot Grant, J.O. Galante MD, DMSc Chair of Orthopedic Surgery (Rush University Medical Center, Chicago, IL), and The Grainger Foundation (Lake Forest, IL).The authors thank the Research Coordinators and nurses for obtaining consent from the participating patients and for collecting peripheral blood samples.

AUTHOR CONTRIBUTIONS

All authors were involved in drafting the manuscript or critically revising it for important intellectual content, and all authors approved the final version to be submitted for publication. In addition to the daily/weekly discussions and study design, analysis of different data and/or patient selection, the authors were more specifically involved in study conception and design (T.A.R, T.T.G and K.M), acquisition of the data (T.B, J.K, B.T, A.K., T.A.R, K.M, T.T.G, J.G, G.S, Z.S, R.S.K and J.A.B), patient selection (J.G, Z.S, J.A.B and R.S.K), and analysis and interpretation of the data (T.T.G, T.B, J.K, A.K, J.G, G.S, Z.S, G.H, R.S.K, B.T, K.M and T.A.R). T.A.R and T.T.G had full access to all of the data and take responsibility for the integrity of the data and the accuracy of the data analysis.

DISCLOSURE

The authors declare no competing financial interests.

Figure legends:

Figure 1. Arthritis-associated changes in the expression of chromatin-modifying enzymes in arthritic mice. **(A)** Heatmap of the expression changes in the mouse spleen cells (representative experiment of three assays). The red squares refer to the upregulated genes and the green squares indicate the downregulated genes. RNA samples from the PGIA mice were compared to the control (adjuvant-injected) mice. The upregulated genes are A04-05, A09, B07-08 and E02; the downregulated genes are A11-12, B01, B09, C03, C10 and C12. See the corresponding genes in **Supplementary Table 2**. **(B)** qRT-PCR analysis of Aurora kinase A (Aurka) and B (Aurkb) expression in the B cells of mice with PGIA and the control (ctrl, adjuvant-injected) mice (n=6). Measured C_t values were normalized to the Gapdh values. **(C)** Immuno-detection (Western blot) of the Aurora kinases. **(D)** Histone H3 phosphorylation levels (H.H3-P) in the B cells of mice with PGIA. Western blot panels represent one of three independent experiments. Mean ± SEM values and levels of significance (** $P < 0.01$) are indicated.

Figure 2. Altered expression of chromatin-modifying enzymes in RA patients. (**A)** Heatmap of gene expression changes in PBMC isolated from treatment-naive RA patients (n=3) compared to age- and gender-matched healthy control individuals. The upregulated genes are A04-05, B06, B10, C08, C11, E03 and E10; the downregulated genes are B03, B08, D01, F11 and G03. Positions and corresponding names of the genes are listed in **Supplementary Table 2**. qRT-PCR analysis of RNA samples that were isolated from (**B)** treatment-naïve (n=15) and **C,** MTX-treated (n=10) RA patients. Measured C_t values were normalized to *β-ACTIN* (panels **B** and **C**). The expression levels of Aurora kinases A and B and were compared to age- and gender-matched healthy controls (n=8). Note, the white columns for *AURKA* and *AURKB* on panels B and C represent the same expression values, the relative expressions were compared to newly diagnosed treatment-naïve (B, black columns) or MTX-treated RA patients (**C,** striated columns). Mean ± SEM values and levels of significance (* $P<0.05$,** $P<0.01$) are indicated.

Figure 3. The expression of Aurora kinase A (Aurka) and B (Aurkb) in mice with PGIA or CIA. **(A and B)** The changes in the Aurora kinase expression profiles were measured by qRT-PCR in B cells isolated from BALB/c mice after repeated immunization with PG (solid line) or type II collagen (CII) (broken line) (n=6). **(C and D)** Changes in the expression profile of the Aurora kinases in the B cells of DBA/1J mice with CIA and PG. The solid line represents kinase expression after CII immunization, and the broken line represents the expression level of Aurora kinases after PG immunization (n=6). The arrows indicate the time of immunization. **(E)** The expression of the Aurora kinases during the development and progression of PGIA in BALB/c mice. The clinical symptoms of arthritis appeared 9-10 days after the 3^{rd} immunization. The arrows indicate the time of immunization with the PG antigen in the DDA adjuvant. DDA-injected BALB/c mice were used as controls (Ctrl). RNA samples were isolated from B cells from 3-4 mice for each time point. Measured C_t values were normalized to *β-actin* gene control in qRT-PCR experiments. Mean ± SEM values and levels of significance (*P <0.05, **P<0.01) are indicated.

Figure 4. Preventive VX-680 treatment of mice immunized with cartilage PG (PGIA). **(A)** Mice (n=10 in each group at each time point). Treatment started 4 days after the third PG injection six days before the expected onset of arthritis. Mice were treated with 40 mg/kg VX-680 or with the vehicle alone (controls) for two weeks (n=10 in each group). The arrows indicate the days of treatment. **(B)** Gene expression of the Aurora kinases (Aurka and Aurkb) was quantified using qRT-PCR. C_t values were normalized with the internal *β-actin* control C_t values. Expression levels in vehicle-treated control animals were considered as 1-fold expression. **(C)** Immunodetection of the Aurora kinase (Aurka and Aurkb) and histone H3 phosphorylation (H.H3-P) level changes in B cells. Western blot panels show one representative sample of three independent experiments. *Gapdh* and *histone H3* (H.H3) were used as loading controls. Mean ± SEM values and levels of significance (*P<0.05, **P<0.01) are indicated.

Figure 5. Therapeutic treatment of established PGIA. **(A)** Arthritic mice (n=9 in each group at each time point) with less than 2 days of the onset of symptoms (mean 2.5 arthritis score) were grouped and were either untreated or treated with 50 mg/kg VX-680 for 10 days. Arthritic ankle and wrist joints were measured using a microcaliper (11) and the cumulative changes for each animal were plotted against the days of the experiment (*x*-axis). The arrows indicate the day of treatment. **(B)** B cells were purified from vehicle-treated control (gray bars) and VX-680 treated (black bars) BALB/c mice with PGIA (n=4 in each group) on day 11 of treatment C_t values were normalized with the internal *β-actin* control C_t values. Expression levels in vehicle-treated, control animals were considered as 1-fold expression. **(C)** Histone fractions from B cells were probed with an anti-histone H3 Ser-10 (H.H3-P) antibody. Unphosphorylated histone H3 (H.H3) was the loading control in these Western blot experiments. Western blot represents one of three independent experiments. Mean ± SEM values and levels of significance (*P<0.05, **P<0.01) are indicated.

Figure 6. Treatment of arthritic mice with VX-680 promotes B lymphocyte apoptosis and reduces B cell numbers in the spleen and bone marrow. **(A-D**) Caspase 3-mediated apoptosis of lymphocytes, isolated from the spleens of control (vehicle-treated) and VX-680-treated arthritic mice on day 11 of treatment (see Fig.5, panel A), was investigated using flow cytometry. **(A** and **B)** B cells were labeled with anti-CD19 antibody, permeabilized, and stained for intracellular active caspase 3. **(C** and **D)** Intracellular active caspase 3 was similarly analyzed in $CD3^+$ spleen T cells. **(E-G)** B1 and B2 cell subsets were further analyzed in the **E**, spleens, **F**, joint draining lymph nodes, and **G**, bone marrow of vehicle-treated and VX-680-treated mice. The percentages of B1 (IgM high/IgD low) and B2 (IgD high/IgM low) subsets were determined by flow cytometry after surface staining of lymphocytes with anti-CD19, anti-IgM, and anti-IgD antibodies, and gating on $CD19^+$ cells. Flow cytometry panels represent one of 3-5 independent experiments.

Reference List

(1) Turesson C, O'Fallon WM, Crowson CS, Gabriel SE, Matteson EL. Extra-articular disease manifestations in rheumatoid arthritis: incidence trends and risk factors over 46 years. Ann Rheum Dis 2003; 62:722-7.

(2) Ballestar E. Epigenetic alterations in autoimmune rheumatic diseases. Nat Rev Rheumatol 2011; 7:263-71.

(3) Jacobi AM, Dorner T. Current aspects of anti-CD20 therapy in rheumatoid arthritis. Curr Opin Pharmacol 2010; 10:316-21.

(4) Chi P, Allis CD, Wang GG. Covalent histone modifications--miswritten, misinterpreted and mis-erased in human cancers. Nat Rev Cancer 2010; 10:457-69.

(5) Carmena M, Ruchaud S, Earnshaw WC. Making the Auroras glow: regulation of Aurora A and B kinase function by interacting proteins. Curr Opin Cell Biol 2009; 21:796-805.

(6) Dar AA, Goff LW, Majid S, Berlin J, El-Rifai W. Aurora kinase inhibitors--rising stars in cancer therapeutics? Mol Cancer Ther 2010; 9:268-78.

(7) Crosio C, Fimia GM, Loury R, Kimura M, Okano Y, Zhou H et al. Mitotic phosphorylation of histone H3: spatio-temporal regulation by mammalian Aurora kinases. Mol Cell Biol 2002; 22:874-85.

(8) Mikecz K, Glant TT, Poole AR. Immunity to cartilage proteoglycans in BALB/c mice with progressive polyarthritis and ankylosing spondylitis induced by injection of human cartilage proteoglycan. Arthritis Rheum 1987; 30:306-18.

(9) Glant TT, Mikecz K. Proteoglycan aggrecan-induced arthritis: a murine autoimmune model of rheumatoid arthritis. Methods Mol Med 2004; 102:313-38.

(10) Glant TT, Radacs M, Nagyeri G, Olasz K, Laszlo A, Boldizsar F et al. Proteoglycan-induced arthritis and recombinant human proteoglycan aggrecan G1 domain-induced arthritis in BALB/c mice resembling two subtypes of rheumatoid arthritis. Arthritis Rheum 2011; 63:1312-21.

(11) Mikecz K, Brennan FR, Kim JH, Glant TT. Anti-CD44 treatment abrogates tissue oedema and leukocyte infiltration in murine arthritis. Nat Med 1995; 1:558-63.

(12) Adarichev VA, Valdez JC, Bardos T, Finnegan A, Mikecz K, Glant TT. Combined autoimmune models of arthritis reveal shared and independent qualitative (binary) and quantitative trait loci. J Immunol 2003; 170:2283-92.

(13) Myers LK, Seyer JM, Stuart JM, Kang AH. Suppression of murine collagen-induced arthritis by nasal administration of collagen. Immunology 1997; 90:161-4.

(14) Glant TT, Adarichev VA, Nesterovitch AB, Szanto S, Oswald JP, Jacobs JJ et al. Disease-associated qualitative and quantitative trait loci in proteoglycan-induced arthritis and collagen-induced arthritis. Am J Med Sci 2004; 327(4):188-95.

(15) Yang D, Liu H, Goga A, Kim S, Yuneva M, Bishop JM. Therapeutic potential of a synthetic lethal interaction between the MYC proto-oncogene and inhibition of aurora-B kinase. Proc Natl Acad Sci U S A 2010; 107:13836-41.

(16) Taylor S, Wakem M, Dijkman G, Alsarraj M, Nguyen M. A practical approach to RT-qPCR-Publishing data that conform to the MIQE guidelines. Methods 2010; 50:S1-S5.

(17) Tate CM, Lee JH, Skalnik DG. CXXC finger protein 1 contains redundant functional domains that support embryonic stem cell cytosine methylation, histone methylation, and differentiation. Mol Cell Biol 2009; 29:3817-31.

(18) Boldizsar F, Kis-Toth K, Tarjanyi O, Olasz K, Hegyi A, Mikecz K et al. Impaired activation-induced cell death promotes spontaneous arthritis in antigen (cartilage proteoglycan)-specific T cell receptor-transgenic mice. Arthritis Rheum 2010; 62(10):2984-94.

(19) Aletaha D, Neogi T, Silman AJ, Funovits J, Felson DT, Bingham CO, III et al. 2010 rheumatoid arthritis classification criteria: an American College of Rheumatology/European League Against Rheumatism collaborative initiative. Ann Rheum Dis 2010; 69:1580-8.

(20) Beck IM, Vanden Berghe W, Vermeulen L, Bougarne N, Vander CB, Haegeman G et al. Altered subcellular distribution of MSK1 induced by glucocorticoids contributes to NF-kappaB inhibition. EMBO J 2008; 27:1682-93.

(21) Mercurio F, Zhu H, Murray BW, Shevchenko A, Bennett BL, Li J et al. IKK-1 and IKK-2: cytokine-activated IkappaB kinases essential for NF-kappaB activation. Science 1997; 278:860-6.

(22) Angyal A, Egelston C, Kobezda T, Olasz K, Laszlo A, Glant TT et al. Development of proteoglycan-induced arthritis depends on T cell-supported autoantibody production, but does not involve significant influx of T cells into the joints. Arthritis Res Ther 2010; 12:R44.

(23) Cantaert T, Kolln J, Timmer T, van der Pouw Kraan TC, Vandooren B, Thurlings RM et al. B lymphocyte autoimmunity in rheumatoid synovitis is independent of ectopic lymphoid neogenesis. J Immunol 2008; 181:785-94.

(24) Dorner T, Radbruch A, Burmester GR. B-cell-directed therapies for autoimmune disease. Nat Rev Rheumatol 2009; 5:433-41.

(25) Kotzin BL. The role of B cells in the pathogenesis of rheumatoid arthritis. J Rheumatol Suppl 2005; 73:14-8.

(26) Harrington EA, Bebbington D, Moore J, Rasmussen RK, Ajose-Adeogun AO, Nakayama T et al. VX-680, a potent and selective small-molecule inhibitor of the Aurora kinases, suppresses tumor growth in vivo. Nat Med 2004; 10(3):262-7.

(27) Gizatullin F, Yao Y, Kung V, Harding MW, Loda M, Shapiro GI. The Aurora kinase inhibitor VX-680 induces endoreduplication and apoptosis preferentially in cells with compromised p53-dependent postmitotic checkpoint function. Cancer Res 2006; 66(15):7668-77.

(28) Yu J, Wang Z, Kinzler KW, Vogelstein B, Zhang L. PUMA mediates the apoptotic response to p53 in colorectal cancer cells. Proc Natl Acad Sci U S A 2003; 100(4):1931-6.

(29) Karouzakis E, Gay RE, Gay S, Neidhart M. Epigenetic control in rheumatoid arthritis synovial fibroblasts. Nat Rev Rheumatol 2009; 5(5):266-72.

(30) Karouzakis E, Gay RE, Michel BA, Gay S, Neidhart M. DNA hypomethylation in rheumatoid arthritis synovial fibroblasts. Arthritis Rheum 2009; 60(12):3613-22.

(31) Huber LC, Brock M, Hemmatazad H, Giger OT, Moritz F, Trenkmann M et al. Histone deacetylase/acetylase activity in total synovial tissue derived from rheumatoid arthritis and osteoarthritis patients. Arthritis Rheum 2007; 56(4):1087-93.

(32) Meinecke I, Cinski A, Baier A, Peters MA, Dankbar B, Wille A et al. Modification of nuclear PML protein by SUMO-1 regulates Fas-induced apoptosis in rheumatoid arthritis synovial fibroblasts. Proc Natl Acad Sci U S A 2007; 104(12):5073-8.

(33) Ospelt C, Gay S. The role of resident synovial cells in destructive arthritis. Best Pract Res Clin Rheumatol 2008; 22(2):239-52.

(34) Wolter S, Doerrie A, Weber A, Schneider H, Hoffmann E, von der OJ et al. c-Jun controls histone modifications, NF-kappaB recruitment, and RNA polymerase II function to activate the ccl2 gene. Mol Cell Biol 2008; 28:4407-23.

(35) Levy D, Kuo AJ, Chang Y, Schaefer U, Kitson C, Cheung P et al. Lysine methylation of the NF-kappaB subunit RelA by SETD6 couples activity of the histone methyltransferase GLP at chromatin to tonic repression of NF-kappaB signaling. Nat Immunol 2011; 12(1):29-36.

(36) Levy D, Liu CL, Yang Z, Newman AM, Alizadeh AA, Utz PJ et al. A proteomic approach for the identification of novel lysine methyltransferase substrates. Epigenetics Chromatin 2011; 4:19.

(37) Villagra A, Cheng F, Wang HW, Suarez I, Glozak M, Maurin M et al. The histone deacetylase HDAC11 regulates the expression of interleukin 10 and immune tolerance. Nat Immunol 2009; 10:92-100.

(38) Satoh T, Takeuchi O, Vandenbon A, Yasuda K, Tanaka Y, Kumagai Y et al. The Jmjd3-Irf4 axis regulates M2 macrophage polarization and host responses against helminth infection. Nat Immunol 2010; 11:936-44.

(39) Jeon YJ, Lee KY, Cho YY, Pugliese A, Kim HG, Jeong CH et al. Role of NEK6 in tumor promoter-induced transformation in JB6 C141 mouse skin epidermal cells. J Biol Chem 2010; 285:28126-33.

(40) Kishimoto T. IL-6: from its discovery to clinical applications. Int Immunol 2010; 22:347-52.

(41) Mori T, Miyamoto T, Yoshida H, Asakawa M, Kawasumi M, Kobayashi T et al. IL-1beta and TNFalpha-initiated IL-6-STAT3 pathway is critical in mediating inflammatory cytokines and RANKL expression in inflammatory arthritis. Int Immunol 2011; 23:701-12.

(42) Leandro MJ, Becerra-Fernandez E. B-cell therapies in established rheumatoid arthritis. Best Pract Res Clin Rheumatol 2011; 25:535-48.

(43) Nakken B, Munthe LA, Konttinen YT, Sandberg AK, Szekanecz Z, Alex P et al. B-cells and their targeting in rheumatoid arthritis--current concepts and future perspectives. Autoimmun Rev 2011; 11:28-34.

(44) Yazici Y. Long-term safety of methotrexate in the treatment of rheumatoid arthritis. Clin Exp Rheumatol 2010; 28:S65-S67.

(45) Albrecht K, Muller-Ladner U. Side effects and management of side effects of methotrexate in rheumatoid arthritis. Clin Exp Rheumatol 2010; 28:S95-101.

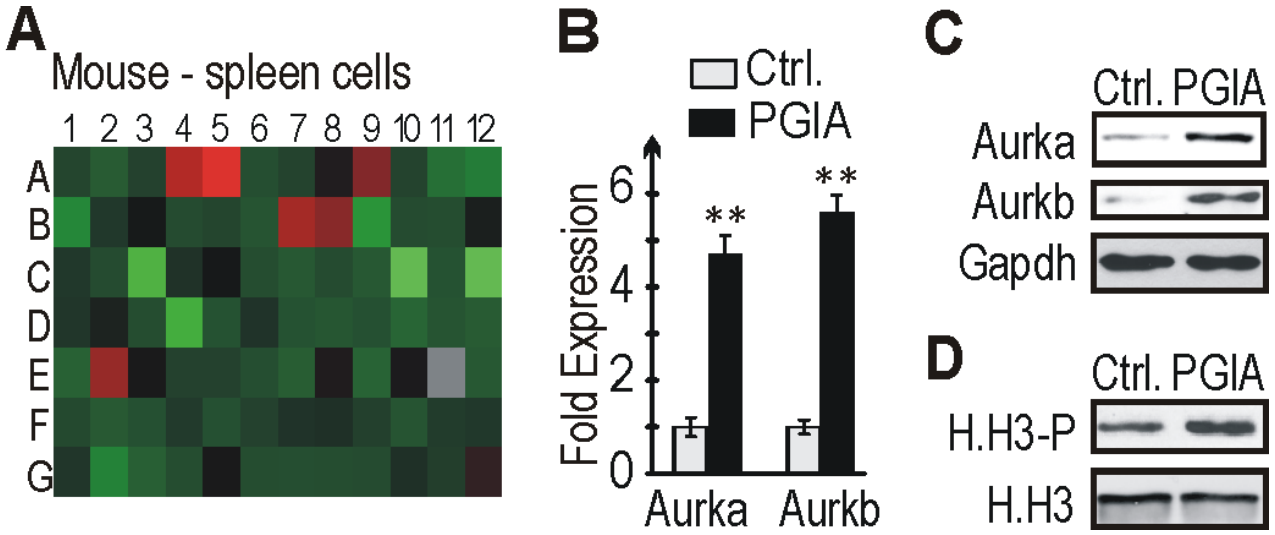

Figure 1. Arthritis-associated changes in the expression of chromatin-modifying enzymes in arthritic mice. (**A)** Heatmap of the expression changes in the mouse spleen cells (representative experiment of three assays). The red squares refer to the upregulated genes and the green squares indicate the downregulated genes. RNA samples from the PGIA mice were compared to the control (adjuvant-injected) mice. The upregulated genes are A04-05, A09, B07-08 and E02; the downregulated genes are A11-12, B01, B09, C03, C10 and C12. See the corresponding genes in **Supplementary Table 1**. (**B)** qRT-PCR analysis of Aurora kinase A (Aurka) and B (Aurkb) expression in the B cells of mice with PGIA and the control (ctrl, adjuvant-injected) mice (n=6). Measured C_t values were normalized to the Gapdh values. (**C)** Immuno-detection (Western blot) of the Aurora kinases. (**D)** Histone H3 phosphorylation levels (H.H3-P) in the B cells of mice with PGIA. Western blot panels represent one of three independent experiments. Mean ± SEM values and levels of significance (** $P < 0.01$) are indicated.

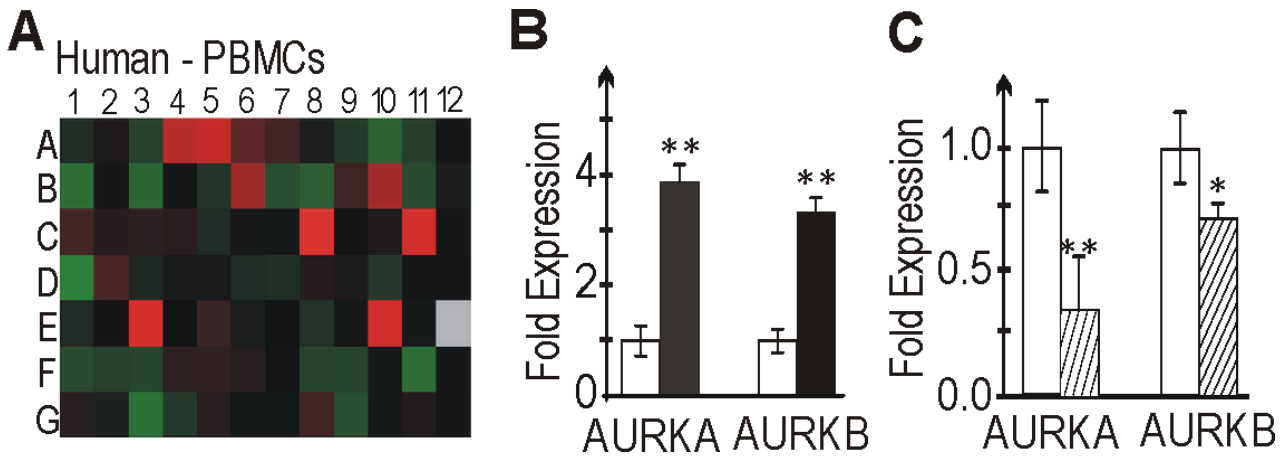

Figure 2. Altered expression of chromatin-modifying enzymes in RA patients. (**A)** Heatmap of gene expression changes in PBMC isolated from treatment-naive RA patients (n=3) compared to age- and gender-matched healthy control individuals. The upregulated genes are A04-05, B06, B10, C08, C11, E03 and E10; the downregulated genes are B03, B08, D01, F11 and G03. Positions and corresponding names of the genes are listed in **Supplementary Table 1**. qRT-PCR analysis of RNA samples that were isolated from (**B)** treatment-naïve (n=15) and **C,** MTX-treated (n=10) RA patients. Measured C_t values were normalized to *β-ACTIN* (panels **B** and **C**).-The expression levels of Aurora kinases A and B and were compared to age- and gender-matched healthy controls (n=8). Note, the white columns for *AURKA* and *AURKB* on panels B and C represent the same expression values, the relative expressions were compared to newly diagnosed treatment-naïve (B, black columns) or MTX-treated RA patients (**C,** striated columns). Mean ± SEM values and levels of significance (* P<0.05,** P<0.01) are indicated.

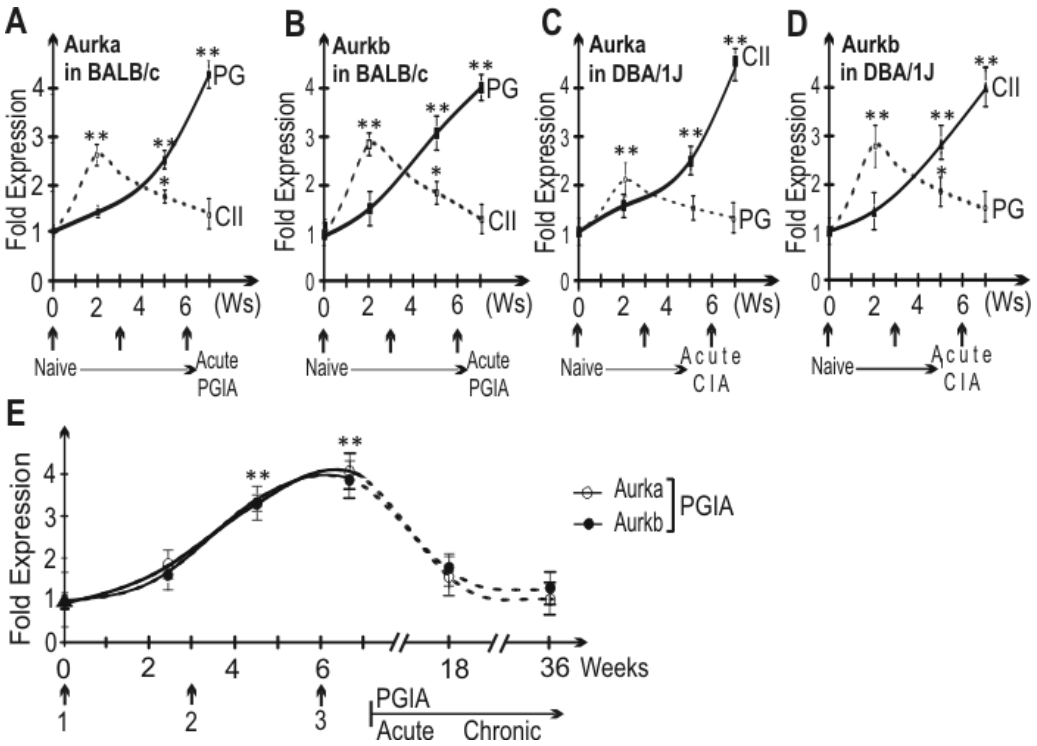

Figure 3. The expression of Aurora kinase A (Aurka) and B (Aurkb) in mice with PGIA or CIA. **(A and B)** The changes in the Aurora kinase expression profiles were measured by qRT-PCR in B cells isolated from BALB/c mice after repeated immunization with PG (solid line) or type II collagen (CII) (broken line) (n=6). **(C and D)** Changes in the expression profile of the Aurora kinases in the B cells of DBA/1J mice with CIA and PG. The solid line represents kinase expression after CII immunization, and the broken line represents the expression level of Aurora kinases after PG immunization (n=6). The arrows indicate the time of immunization. **(E)** The expression of the Aurora kinases during the development and progression of PGIA in BALB/c mice. The clinical symptoms of arthritis appeared 9-10 days after the 3rd immunization. The arrows indicate the time of immunization with the PG antigen in the DDA adjuvant. DDA-injected BALB/c mice were used as controls (Ctrl). RNA samples were isolated from B cells from 3-4 mice for each time point. Measured C_t values were normalized to *β-actin* gene control in qRT-PCR experiments. Mean ± SEM values and levels of significance (*P <0.05, **P<0.01) are indicated.

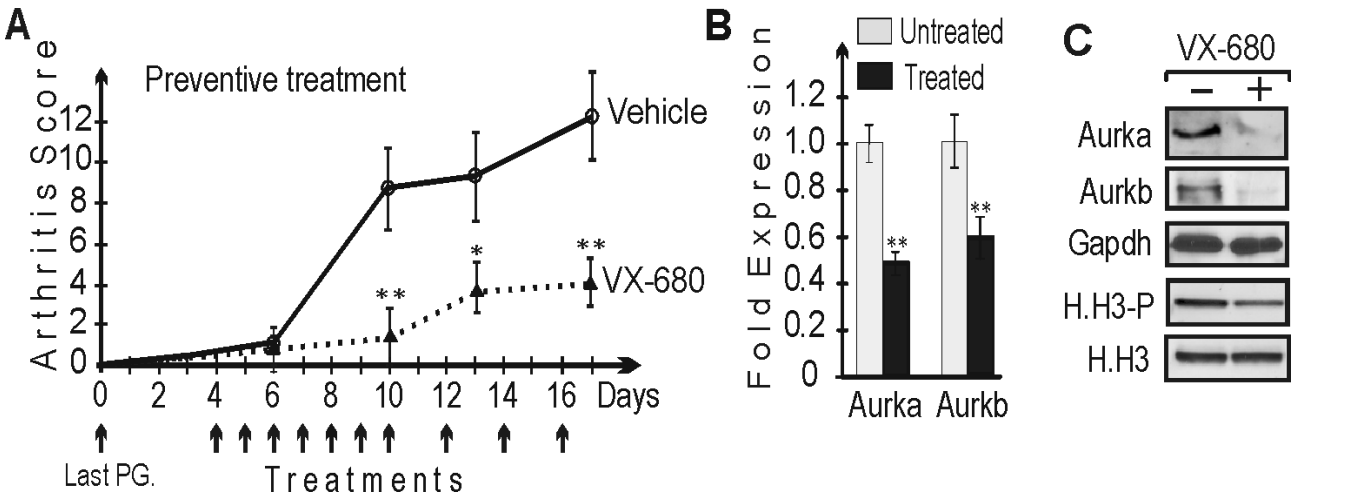

Figure 4. Preventive VX-680 treatment of mice immunized with cartilage PG (PGIA). **(A)** Mice (n=10 in each group at each time point). Treatment started 4 days after the third PG injection six days before the expected onset of arthritis. Mice were treated with 40 mg/kg VX-680 or with the vehicle alone (controls) for two weeks (n=10 in each group). The arrows indicate the days of treatment. **(B)** Gene expression of the Aurora kinases (Aurka and Aurkb) was quantified using qRT-PCR. C_t values were normalized with the internal *β-actin* control C_t values. Expression levels in vehicle-treated control animals were considered as 1-fold expression. **(C)** Immunodetection of the Aurora kinase (Aurka and Aurkb) and histone H3 phosphorylation (H.H3-P) level changes in B cells. Western blot panels show one representative sample of three independent experiments. *Gapdh* and *histone H3* (H.H3) were used as loading controls. Mean ± SEM values and levels of significance (*P<0.05, **P<0.01) are indicated.

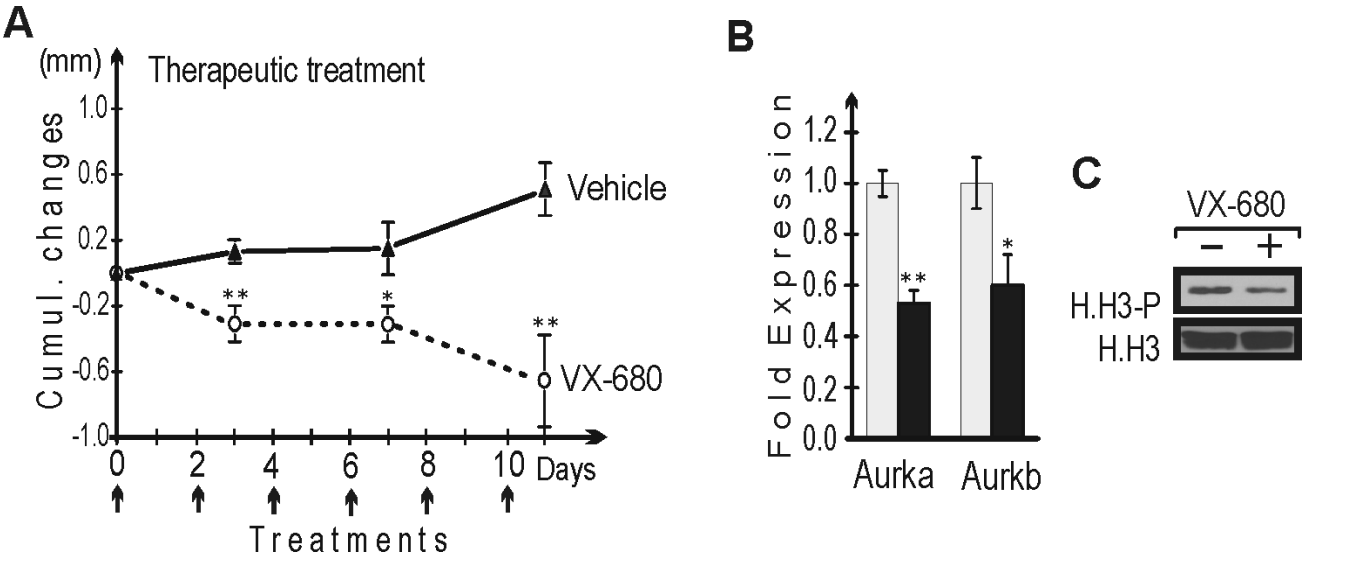

Figure 5. Therapeutic treatment of established PGIA. **(A)** Arthritic mice (n=9 in each group at each time point) with less than 2 days of the onset of symptoms (mean 2.5 arthritis score) were grouped and were either untreated or treated with 50 mg/kg VX-680 for 10 days. Arthritic ankle and wrist joints were measured using a microcaliper (11) and the cumulative changes for each animal were plotted against the days of the experiment (*x*-axis). The arrows indicate the day of treatment. **(B)** B cells were purified from vehicle-treated control (gray bars) and VX-680 treated (black bars) BALB/c mice with PGIA (n=4 in each group) on day 11 of treatment C_t values were normalized with the internal *β-actin* control C_t values. Expression levels in vehicle-treated, control animals were considered as 1-fold expression. **(C)** Histone fractions from B cells were probed with an anti-histone H3 Ser-10 (H.H3-P) antibody. Unphosphorylated histone H3 (H.H3) was the loading control in these Western blot experiments. Western blot represents one of three independent experiments. Mean ± SEM values and levels of significance (*P<0.05, **P<0.01) are indicated.

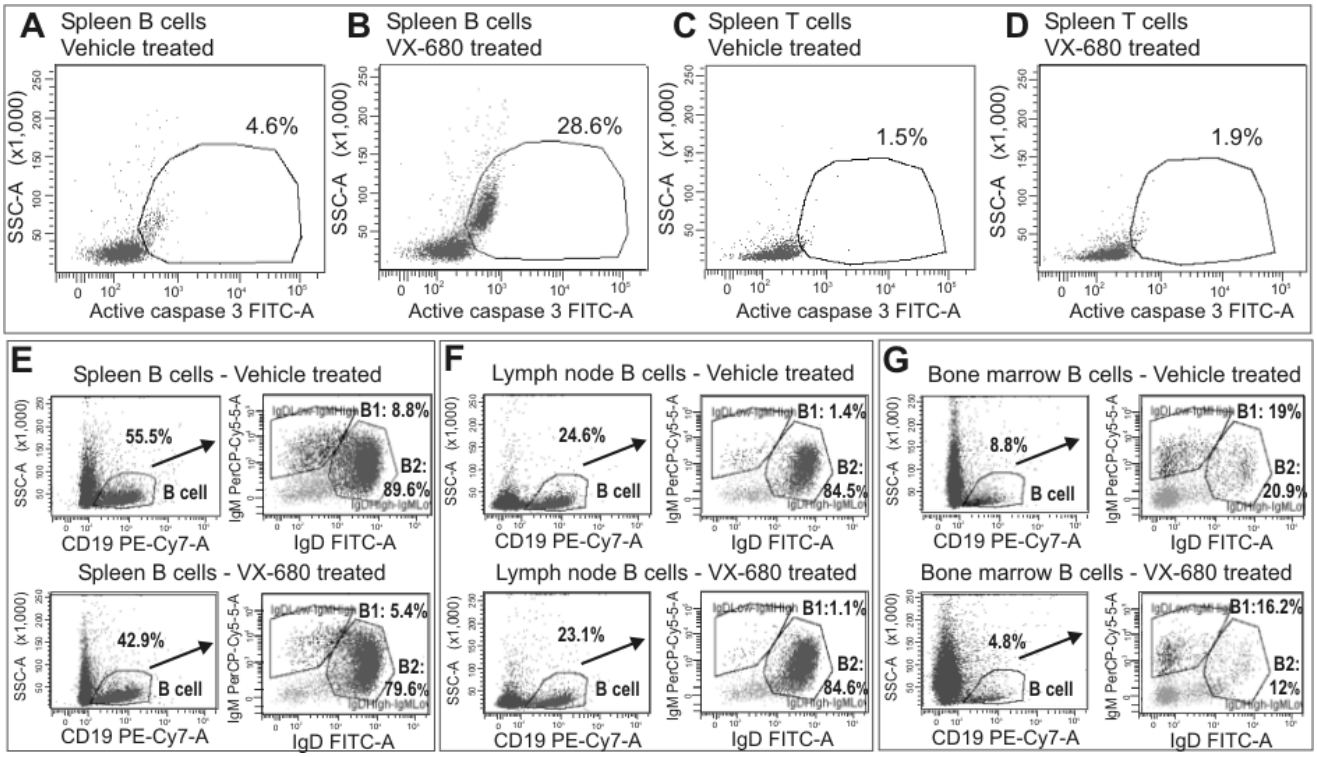

Figure 6. Treatment of arthritic mice with VX-680 promotes B lymphocyte apoptosis and reduces B cell numbers in the spleen and bone marrow. **(A-D**) Caspase 3-mediated apoptosis of lymphocytes, isolated from the spleens of control (vehicle-treated) and VX-680-treated arthritic mice on day 11 of treatment (see Fig.5, panel A), was investigated using flow cytometry. (**A** and **B)** B cells were labeled with anti-CD19 antibody, permeabilized, and stained for intracellular active caspase 3. (**C** and **D)** Intracellular active caspase 3 was similarly analyzed in $CD3^+$ spleen T cells. (**E-G)** B1 and B2 cell subsets were further analyzed in the **E**, spleens, **F**, joint draining lymph nodes, and **G**, bone marrow of vehicle-treated and VX-680-treated mice. The percentages of B1 (IgM high/IgD low) and B2 (IgD high/IgM low) subsets were determined by flow cytometry after surface staining of lymphocytes with anti-CD19, anti-IgM, and anti-IgD antibodies, and gating on $CD19^+$ cells. Flow cytometry panels represent one of 3-5 independent experiments.

Supplementary Table 1. RA patients and healthy control individuals involved in the experiments

Subjects	Patient Code:	Gender	Age	ACPA	RF	TTS
DMARD naïve	BA-11	F	58	−	−	T.N.
	BI-11	F	73	−	+	T.N.
	EI-11	F	30	+	−	T.N.
	FI-11	F	57	+	−	T.N.
	FMG-11	F	49	+	−	T.N.
	KA-11	F	43	+	+	T.N.
	ML-11	F	63	+	+	T.N.
	NK-12	F	56	+	−	T.N.
	UJ-12	M	68	+	+	T.N.
	TS-11	M	35	+	+	SASP
	KN-10	F	20	−	−	SASP
	MT-10	F	67	−	−	SASP
	SV-10	M	31	−	−	STE
	EPJ-10	F	51	−	−	NSAID
	PP-10	M	47	−	−	HCQ
	LLI-11	F	58	−	−	NSAID, STE
MTX-treated	KJ-10	F	61	+	−	MTX
	VL-11	F	48	+	+	MTX
	BE-11	M	94	−	−	MTX
	DD-11	F	22	−	−	MTX
	KJ-11	F	61	−	−	MTX
	BJ-11	F	54	−	−	MTX
	OE-11	F	22	+	+	MTX
	KF-11	M	55	+	+	MTX
	GI-11	F	59	+	+	MTX
	MJ-11	F	58	+	+	MTX
Controls	AA-10	F	60+	N/A	N/A	N/A
	BB-10	M	60+	N/A	N/A	N/A
	CC-10	F	50+	N/A	N/A	N/A
	DD-10	M	50+	N/A	N/A	N/A
	EE-10	F	40+	N/A	N/A	N/A
	FF-11	M	40+	N/A	N/A	N/A
	GG-11	F	30+	N/A	N/A	N/A
	HH-11	M	30+	N/A	N/A	N/A

TTS - Treatment at the time of sampling
T. N. – Treatment-naive
ACPA - Anti-Cyclic Citrullinated Peptide positive if ACPA >25 U/ml
RF - Rheumatoid factor positive if RF >50 U/ml
SASP - Sulphasalazine
STE - Steroid
NSAID - Non-steroidal anti-inflammatory drug
HCQ – Hydroxychloroquine
NSAID – Non-steroid anti-inflammatory drug
MTX - Methotrexate

Supplementary Table 2. Mouse and human PCR arrays of chromatin-modifying enzymes

Table 2A: Mouse data

Array Position	Gene Symbol	Fold up- or down- Regulation		
		Spleen	B cells	T cells
A01	Kdm1	-1.4	-1.56	-1.24
A02	Ash1l	-1.71	-1.87	-1.56
A03	Atf2	-1.43	-1.52	-1.34
A04	**Aurka**	**3.17**	**3.65**	**2.5**
A05	**Aurkb**	**4.44**	**6.01**	**2.41**
A06	Aurkc	-1.82	-1.68	-1.76
A07	Carm1	-1.53	-1.55	-1.11
A08	Cdyl	1.32	1.35	1.05
A09	**Ciita**	**2.58**	**2.62**	**1.55**
A10	Csrp2bp	-1.49	-1.55	-1.23
A11	**Dnmt1**	**-2.37**	**-2.15**	**-1.99**
A12	**Dnmt3a**	**-1.83**	**-2.35**	**-2.23**
B01	**Dnmt3b**	**-1.79**	**-2.55**	**-1.21**
B02	Dot1l	-1.57	-1.43	-1.55
B03	Dzip3	-1.12	-1.1	-1.24
B04	Ehmt1	-1.63	-1.64	-1.21
B05	Ehmt2	-1.72	-1.56	-1.14
B06	Esco1	-1.15	-1.77	-1.18
B07	**Esco2**	**2.85**	**3.31**	**1.92**
B08	**Hat1**	**2.88**	**2.73**	**1.98**
B09	**Hdac1**	**-2.73**	**-2.81**	**-1.88**
B10	Hdac10	-1.45	-1.64	-1.66
B11	Hdac11	-1.67	-1.65	-1.29
B12	Hdac2	-1.14	-1.17	-1.37
C01	Hdac3	-1.67	-1.42	-1.45
C02	Hdac4	-1.78	-1.64	-1.67
C03	**Hdac5**	**-3.36**	**-3.84**	**-2.34**
C04	Hdac6	-1.31	-1.34	-1.28
C05	Hdac7	1.52	1.19	1.34
C06	Hdac8	-1.27	-1.66	-1.45
C07	Hdac9	-1.45	-1.82	-1.91

Table 2B: Human data

Array Position	Gene Symbol	Fold up- or down- Regulation			Mean±SEM	Significance (2-tailed)
		RA-1	RA-2	RA-3		
A01	KDM1A	-2.03	-1.42	-1.13	-1.52±0.26	$P < 0.05$
A02	ASH1L	-1.24	1.39	1.9	0.68±0.97	N.s.
A03	ATF2	-3.46	-1.72	-2.83	-2.67±0.5	$P < 0.05$
A04	**AURKA**	**13.36**	**7.15**	**24.95**	**15.13±5.22**	***P* < 0.05**
A05	**AURKB**	**7.46**	**7.96**	**9.03**	**8.15±0.46**	***P* < 0.05**
A06	AURKC	-1.28	2.69	-4.34	-0.97±2.03	N.s.
A07	CARM1	1.42	2.08	3.21	2.23±0.52	$P < 0.05$
A08	CDYL	-2.06	-1.21	-1.49	-1.58±0.25	$P < 0.05$
A09	CIITA	-6.73	-1.61	-2.87	-3.73±1.5	$P < 0.05$
A10	CSRP2BP	-2.43	-2.4	-1.51	-2.11±0.3	$P < 0.05$
A11	DNMT1	-4.23	-1.66	-2.68	-2.85±0.74	$P < 0.05$
A12	DNMT3A	-1.55	1.14	1.78	0.45±1.02	N.s.
B01	DNMT3B	1.89	-2.67	-10.02	-3.6±3.46	N.s.
B02	DOT1L	1.74	1.2	3.11	2.01±0.56	$P < 0.05$
B03	**DZIP3**	**-2.6**	**-2.49**	**-2**	**-2.36±0.18**	***P* < 0.05**
B04	EHMT2	-3.18	-1.07	-1.46	-1.9±0.64	$P < 0.05$
B05	ESCO1	-2.19	-1.53	-1.61	-1.77±0.2	$P < 0.05$
B06	**ESCO2**	**6.73**	**5.21**	**9.48**	**7.14±1.28**	***P* < 0.05**
B07	HAT1	-1.06	-1.96	-1.12	-1.38±0.29	$P < 0.05$
B08	**HDAC1**	**-2.93**	**-2.28**	**-2.54**	**-2.58±0.18**	***P* < 0.05**
B09	HDAC10	1.27	1.98	2.96	2.07±0.48	$P < 0.05$
B10	**HDAC11**	**5.5**	**5.6**	**10.19**	**7.09±0.54**	***P* < 0.05**
B11	HDAC2	8	-1.89	-1.04	1.69±3.1	N.s.
B12	HDAC3	-1.84	-1.18	-1.8	-1.6±0.21	$P < 0.05$
C01	HDAC4	1.17	2.1	1.97	1.74±0.29	$P < 0.05$
C02	HDAC5	2.35	1.57	-1.04	0.96±1.02	N.s.
C03	HDAC6	-1.83	1.66	2.23	0.68±1.26	N.s.
C04	HDAC7	1.35	1.58	2.74	1.89±0.43	$P < 0.05$
C05	HDAC8	-3.29	-1.37	-1.91	-2.19±0.57	$P < 0.05$
C06	HDAC9	1.68	1.22	2.22	1.7±0.28	$P < 0.05$
C07	KDM5B	-2.38	-1.1	-1.88	-1.78±0.37	$P < 0.05$

C08	Kdm5b	-1.57	-1.63	-1.23	**C08**	**KDM5C**	**12.33**	**12.01**	**21.85**	**15.39±3.22**	***P* < 0.05**
C09	Kdm5c	-1.98	-1.81	-1.46	C09	KDM4A	-3.48	1.02	-1.87	-1.44±1.31	N.s.
C10	**Kdm4a**	**-3.94**	**-4.57**	**-2.32**	C10	KDM4C	-1.69	1.42	1.49	0.4±1.04	N.s.
C11	Kdm4c	-1.62	-1.72	-1.65	**C11**	**KDM6B**	**3.78**	**9.72**	**8.84**	**7.44±1.85**	***P* < 0.05**
C12	**Kdm6b**	**-3.415**	**-4.6**	**-2.23**	C12	KAT2A	-2.39	1.18	1.08	-0.04±0.82	N.s.
D01	Kat2a	-1.75	-1.41	-1.38	**D01**	**KAT2B**	**-3.1**	**-3.19**	**-3.97**	**-3.4±0.27**	***P* < 0.05**
D02	Kat2b	-1.12	-1.21	-1.47	D02	KAT5	1.25	2.2	2.72	2.05±0.43	*P* < 0.05
D03	Kat5	-1.89	-1.65	-1.31	D03	MBD2	-1.98	-1.34	-1.18	-1.5±0.08	*P* < 0.05
D04	**Mll3**	**-3.15**	**-3.61**	**-2.22**	D04	MLL	-2.6	-1.17	-1.36	-1.71±0.44	*P* < 0.05
D05	Mll5	-1.43	-1.72	-1.24	D05	MLL3	-6.41	1.26	-4.01	-3.05±2.26	N.s.
D06	Mysm1	-1.99	-1.36	-1.82	D06	MLL5	-2.13	-1.39	-1.74	-1.75±0.21	*P* < 0.05
D07	Myst1	-1.92	-1.72	-1.67	D07	MYSM1	-1.62	-1.44	-1.17	-1.41±0.13	*P* < 0.05
D08	Myst2	-1.45	-1.78	-1.56	D08	KAT8	1	1.53	1.57	1.36±0.18	N.s.
D09	Myst3	-1.79	-1.7	-1.45	D09	KAT7	1.19	1.38	2.03	1.53±0.25	*P* < 0.05
D10	Myst4	-1.28	-1.99	-1.24	D10	KAT6A	-1.17	-1.58	-1.07	-1.27±0.15	*P* < 0.05
D11	Ncoa1	-1.78	-1.76	-1.36	D11	KAT6B	1.71	1.2	2.18	1.69±0.28	*P* < 0.05
D12	Ncoa3	-1.91	-1.86	-1.96	D12	NCOA1	1.71	1.13	2.06	1.63±0.27	*P* < 0.05
E01	Ncoa6	-2.2	-1.93	-1.31	E01	NCOA3	-1.24	-1.36	1.03	-0.52±0.77	N.s.
E02	**Nek6**	**3.12**	**2.99**	**1.99**	E02	NCOA6	-1.24	1.07	1.04	0.29±0.76	N.s.
E03	Nsd1	1.54	1.22	1.55	**E03**	**NEK6**	**5.94**	**10.27**	**11.91**	**9.37±1.78**	***P* < 0.05**
E04	Pak1	-1.98	-1.52	-1.32	E04	NSD1	-1.21	-1	1.07	-0.38±0.76	N.s.
E05	Prmt1	1.65	-1.52	-1.78	E05	PAK1	1.27	1.93	1.4	1.53±0.2	*P* < 0.05
E06	Prmt2	-1.94	-1.67	-1.45	E06	PRMT1	-1.68	-1.22	1	-0.63±0.82	N.s.
E07	Prmt3	-1.78	-1.89	-1.36	E07	PRMT2	-1.68	-1.02	1.12	-0.52±0.84	N.s.
E08	Prmt5	-1.15	1.32	1.11	E08	PRMT3	-2.04	-1.49	-1.42	-1.65±0.19	*P* < 0.05
E09	Prmt6	-1.15	-1.96	-1.45	E09	PRMT5	-1.06	-1.11	1.39	-0.26±0.82	N.s.
E10	Prmt7	1.47	1.27	1.65	**E10**	**PRMT6**	**7.36**	**9.52**	**17.32**	**11.4±3.02**	***P* < 0.05**
E11	Prmt8	-1.99	-1.53	-1.45	E11	PRMT7	-2.2	-1.13	-1.46	-1.59±0.31	*P* < 0.05
E12	Rnf2	-1.76	-1.81	-1.56	E12	PRMT8	N/A	N/A	N/A	N/A	N/A
F01	Rnf20	-1.98	-1.6	-1.45	F01	RNF2	-2.35	-1.89	-1.71	-1.98±0.19	*P* < 0.05
F02	Rps6ka3	-1.87	-1.84	-1.76	F02	RNF20	-1.65	-1.74	-1.35	-1.58±0.11	*P* < 0.05
F03	Rps6ka5	-1.82	-1.7	-1.34	F03	RPS6KA3	-1.66	-1.79	-1.51	-1.65±0.08	*P* < 0.05
F04	Setd1a	-1.64	-1.44	-1.56	F04	RPS6KA5	-1.43	1.73	1.02	0.44±0.95	N.s.
F05	Setd1b	-1.32	-1.7	-1.65	F05	SETD1A	1.02	1.78	1.76	1.52±0.25	*P* < 0.05
F06	Setd2	-1.85	-1.53	-1.34	F06	SETD1B	1.26	1.62	2.42	1.76±0.34	*P* < 0.05
F07	Setd3	1.56	-1.36	-1.56	F07	SETD2	-1.19	-1.05	1.18	-0.35±0.76	N.s.

F08	Setd4	-1.46	-1.32	-1.89	F08	SETD3	-1.95	-1.78	-1.61	-1.78±0.09	*P* < 0.05
F09	Setd5	-1.33	-1.5	-1.56	F09	SETD4	-2.77	-1.8	-1.66	-2.07±0.34	*P* < 0.05
F10	Setd6	-1.57	-1.76	-1.45	F10	SETD5	-1.89	-1.12	-1.18	-1.39±0.24	*P* < 0.05
F11	Setd7	-1.91	-1.46	-1.56	**F11**	**SETD6**	**-3.29**	**-2.7**	**-2.33**	**-2.77±0.27**	***P* < 0.05**
F12	Setd8	-1.67	-1.43	-1.23	F12	SETD7	-1.93	-1.06	-1.41	-1.46±0.25	*P* < 0.05
G01	Setdb1	-1.75	-1.41	-1.64	G01	SETD8	1.26	1.6	1.86	1.57±0.17	*P* < 0.05
G02	**Setdb2**	**-2.95**	**-2.47**	**-2.28**	G02	SETDB1	-1.51	-1.27	1.07	-0.57±0.82	N.s.
G03	Smyd1	-1.76	-1.91	-1.76	**G03**	**SETDB2**	**-5.39**	**-2.73**	**-4.55**	**-4.22±0.78**	***P* < 0.05**
G04	Smyd3	-1.24	-1.66	-1.35	G04	SMYD3	-1.69	-1.6	-1.61	-1.63±0.02	*P* < 0.05
G05	Suv39h1	1.78	1.21	1.23	G05	SUV39H1	1.07	1.58	2.35	1.66±0.37	*P* < 0.05
G06	Suv420h1	-1.89	-1.65	-1.78	G06	SUV420H1	-2.17	-1.09	-1.53	-1.59±0.31	*P* < 0.05
G07	Ube2a	-1.73	-1.67	-1.19	G07	UBE2A	-1.65	-1.1	-1.47	-1.4±0.16	*P* < 0.05
G08	Ube2b	-1.86	-1.66	-1.87	**G08**	**UBE2B**	**2.64**	**2.08**	**2.92**	**2.54±0.24**	***P* < 0.05**
G09	Usp16	-1.77	-1.63	-1.49	G09	USP16	-1.72	-1.98	-1.41	-1.7±0.16	*P* < 0.05
G10	Usp21	-1.1	-1.33	-1.89	G10	USP21	-1.29	-1.13	1.37	-0.35±0.86	N.s.
G11	Usp22	-1.78	-1.49	-1.23	G11	USP22	-1.31	1.43	1.39	0.5±0.9	N.s.
G12	Whsc1	1.54	1.53	1.65	G12	WHSC1	-1.48	1.16	1.06	0.24±0.86	N.s.

Supplementary Table 1. Mouse and human PCR arrays for gene expression levels of chromatin-modifying enzymes. Table 1A: Mouse PCR array data for spleen B and T cells isolated from mice with PGIA in comparison with control (adjuvant-injected) mice. Table 1B: Human PCR array data for PBMCs isolated from disease-modifying anti-rheumatic drug (DMARD)-naive RA patients compared to PBMCs from control healthy donors. Colored, bold-faced numbers refer to significantly **up**- or **down**regulated gene expression levels that show at least a 2-fold difference. In both array systems, the gene expression of the chromatin-modifying enzymes was normalized to 5 reference genes and fold changes in expression levels are shown relative to the controls. Each column in the mouse panel represents the average from 3 mice. Results from three DMARD treatment-naive RA patients (as compared to three healthy donors) were analyzed using the non-parametric Mann-Whitney U test (SPSS, Chicago, IL). Significant differences ($P < 0.05$) are indicated in the last column (N.s.: Not significant; N/A: Not applicable). These 3 DMARD-naive patients have been included in validation studies (n=15) for AURKA and AURKB expression (Figure 2A and B). Six genes (highlighted with light gray background) differ between the mouse and human PCR array platforms.

Supplementary Table 3: Measured C_t of values of qRT-PCR and calculated (software: RT^2 Profiler PCR Array Data Analysis v3.5) delta C_t values for human studies.

	GENES		Measured Ct		AVG Delta Ct		2^(-Delta Ct)		Fold Expression Changes
			RA-1	Ctrl-1	RA-1	Ctrl-1	RA-1	Ctrl-1	
RA-1 sample	Up-regulated	AURKA	27.34	29.11	0.75	4.49	0.5930	0.0445	13.3
		AURKB	27.56	30.17	1.81	4.71	0.2844	0.0382	7.4
		ESCO2	30.54	33.29	4.93	7.69	0.0327	0.0048	6.7
		HDAC11	26.84	29.87	1.51	3.99	0.3501	0.0629	5.5
		KDM5C	28.16	30.04	1.68	5.31	0.3112	0.0252	12.3
		KDM6B	26.4	29.99	1.63	3.55	0.3222	0.0854	3.7
		NEK6	26.28	29.21	0.85	3.43	0.5532	0.0928	5.9
		PRMT6	29.82	32.45	4.09	6.97	0.0586	0.0080	7.3
		UBE2B	25.05	29.15	0.79	2.2	0.5767	0.2176	2.6
	Down-regulated	DZIP3	28.02	34.46	6.1	4.68	0.0145	0.0390	-2.6
		HDAC1	25.59	32.20	3.84	2.27	0.0696	0.2073	-2.9
		KAT2B	27.70	34.39	6.03	4.45	0.0153	0.0458	-3.1
		SETD6	28.22	35.34	6.64	4.9	0.0100	0.0335	-3.2
		SETDB2	27.05	34.54	6.18	3.75	0.0138	0.0743	-5.3
RA-2 sample	Up-regulated	AURKA	29.00	26.94	1.54	4.39	0.3429	0.0477	7.2
		AURKB	30.85	28.94	3.39	6.38	0.0951	0.0120	7.9
		ESCO2	33.35	30.84	5.89	8.28	0.0168	0.0032	5.2
		HDAC11	33.34	30.94	5.88	8.39	0.0169	0.0030	5.6
		KDM5C	31.35	30.04	3.89	7.49	0.0673	0.0056	12.0
		KDM6B	29.35	27.72	1.89	5.17	0.2691	0.0277	9.7
		NEK6	28.90	27.35	1.44	4.8	0.3675	0.0359	10.2
		PRMT6	31.35	29.70	3.89	7.15	0.0673	0.0070	9.5
		UBE2B	29.18	25.29	1.72	2.74	0.3027	0.1502	2.0
	Down-regulated	DZIP3	34.27	28.06	6.81	5.5	0.0089	0.0220	-2.4
		HDAC1	31.51	25.45	4.05	2.89	0.0602	0.1345	-2.2
		KAT2B	33.57	26.99	6.11	4.44	0.0144	0.0461	-3.1
		SETD6	34.71	28.37	7.25	5.82	0.0066	0.0177	-2.7
		SETDB2	33.29	26.95	5.83	4.39	0.0175	0.0476	-2.7
RA-3 sample	Up-regulated	AURKA	27.68	26.94	-0.25	4.39	1.1876	0.0477	24.9
		AURKB	31.14	28.94	3.21	6.38	0.1079	0.0120	9.0
		ESCO2	32.97	30.84	5.04	8.28	0.0304	0.0032	9.4
		HDAC11	32.97	30.94	5.04	8.39	0.0304	0.0030	10.1
		KDM5C	30.97	30.04	3.04	7.49	0.1214	0.0056	21.8
		KDM6B	29.97	27.72	2.04	5.17	0.2428	0.0277	8.8
		NEK6	29.15	27.35	1.22	4.8	0.4287	0.0359	11.9
		PRMT6	30.96	29.70	3.03	7.15	0.1223	0.0070	17.3
		UBE2B	29.09	25.29	1.16	2.74	0.4469	0.1502	2.9
	Down-regulated.	DZIP3	34.43	28.06	6.5	5.5	0.0110	0.0220	-2.0
		HDAC1	32.17	25.45	4.24	2.89	0.0528	0.1345	-2.5
		KAT2B	34.36	26.99	6.43	4.44	0.0116	0.0461	-3.9
		SETD6	34.95	28.37	7.02	5.82	0.0077	0.0177	-2.3
		SETDB2	34.51	26.95	6.58	4.39	0.0104	0.0476	-4.5

SUPPLEMENTARY INFORMATION

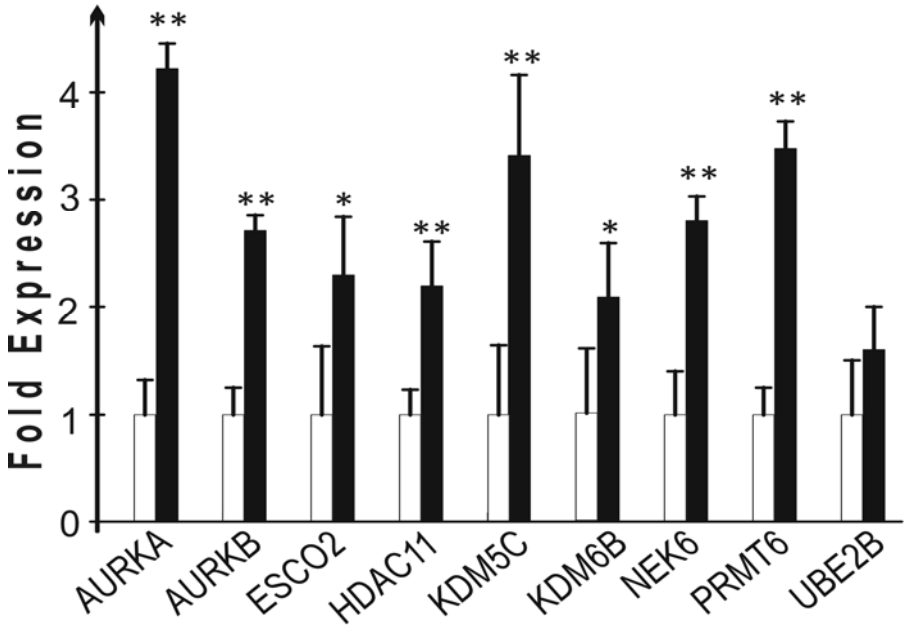

Supplementary Figure 1. Verification of the human PCR array data. RA-specific upregulation of chromatin-modifying enzymes in PBMCs. Total RNA samples were purified from DMARD-naive RA patients (n=3, the same RNA/cDNA samples were used for PCR array, Fig.2A). qRT-PCR Ct values were normalized with the internal *β-ACTIN* gene control Ct value. Black columns represent fold expressions measured in RA patients (n=3), and the white columns represent the age- and gender-matched healthy controls (n=3). Expression levels of the controls were considered as 1-fold expression. Mean ± SEM values and levels of significance (*$P < 0.05$ and **$P < 0.01$) are indicated.

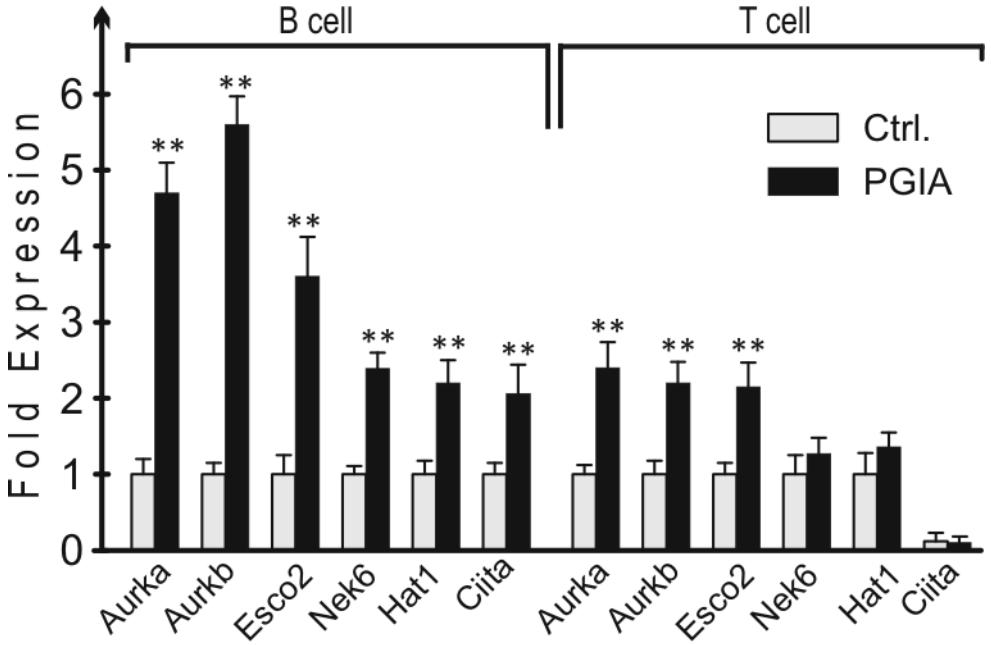

Supplementary Figure 2. PGIA-associated changes in expression of chromatin-modifying enzymes in B and T lymphocytes from mice with PGIA. B and T cells were affinity-purified from control (adjuvant-injected, gray bars) and PG-immunized BALB/c mice (black bars, n=3 in each group). qRT-PCR Ct values were normalized with the internal *β-actin* control Ct values. Measured values from the adjuvant-treated (non-arthritic) control mice were considered as 1-fold expression. Mean ± SEM values and levels of significance (**P < 0.01) are indicated.

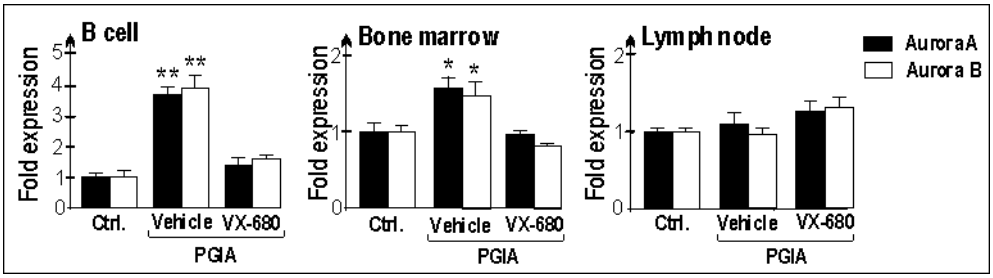

Supplementary Figure 3. Aurora kinase A and B expression in arthritic mice. Total RNA samples was isolated from spleen B lymphocytes, bone marrow and joint draining lymph nodes. qRT-PCR C_t values were normalized to the internal *β-actin* Ct values. Measured values from the adjuvant-treated control (non-arthritic) mice were considered as 1-fold expression. Mean ± SEM values and levels of significance (*P < 0.05 and **P < 0.01) are indicated.

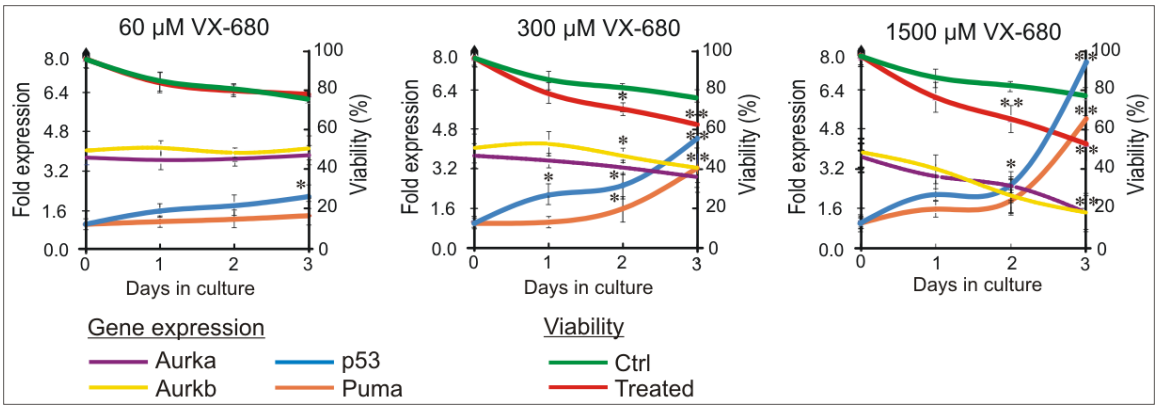

Supplementary Figure 4. VX-680-treatment of spleen cells induces the increased expression of apoptosis-promoting genes. Splenocyte cultures established from arthritic mice were treated with increasing amounts of VX-680 for 3 days, and the expression of *p53, Puma and Aurora* kinese genes were quantified by qRT-PCR (left y axis). Measured C_t values were normalized to the internal *β-actin* C_t value, and the expression rates in the mock-treated control cultures were considered as 1-fold expression. Viability of cells was determined on each day (right y axis). Levels of significance are indicated (*P < 0.05 and **P < 0.01).

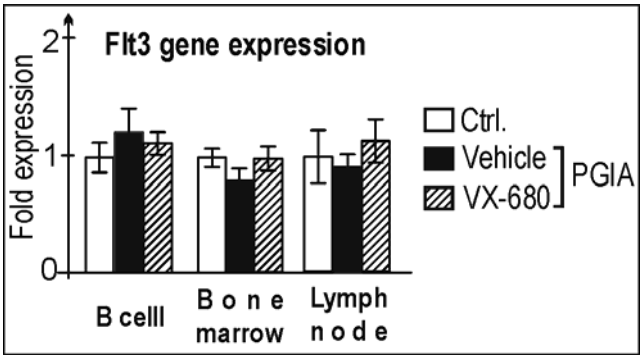

Supplementary Figure 5. Flt3 expression in mice with PGIA. RNA samples were prepared from spleen B cells, and lymphocytes from bone marrow and joint draining lymph nodes of adjuvant-injected (Ctrl), arthritic (PGIA) vehicle-treated, and VX-680-treated arthritic BALB/c mice. The expression of the *Flt3* gene was quantified by qRT-PCR and normalized to *β-actin* control C_t value.